The Effect of Water Glass Content on the Morphology and Thermal Properties of Anorthite-Based Ceramic Foam Filter for Aluminum Alloy Casting

Donanta Dhaneswara
Department of Metallurgical & Materials Engineering, Universitas Indonesia

Iman Abdullah
Department of Chemistry, Universitas Indonesia

Kristanto Wahyudi
Balai Besar Standarisasi dan Pelayanan Jasa Industri Keramik dan Mineral Nonlogam, Ministry of Indusrty

Maulid Purnawan
Balai Besar Standarisasi dan Pelayanan Jasa Industri Keramik dan Mineral Nonlogam, Ministry of Indusrty

他

https://doi.org/10.5109/7326979

出版情報：Evergreen. 11 (4), pp.3431-3438, 2024-12. Interdisciplinary Graduate School of Engineering Sciences, Kyushu University, Japan
バージョン：

The Effect of Water Glass Content on the Morphology and Thermal Properties of Anorthite-based Ceramic Foam Filter for Aluminum Alloy Casting

Donanta Dhaneswara[1,*], Iman Abdullah[2], Kristanto Wahyudi[3], Maulid Purnawan[3], Han Hisyam Pratama[1]

[1]Department of Metallurgical & Materials Engineering, Universitas Indonesia, Depok 16426, Indonesia

[2]Department of Chemistry, Universitas Indonesia, Depok 16426, Indonesia

[3]Balai Besar Standarisasi dan Pelayanan Jasa Industri Keramik dan Mineral Nonlogam, Ministry of Indusrty, Bandung 40272, Indonesia

*Authors to whom correspondence should be addressed:
E-mail: donanta.dhaneswara@ui.ac.id

(Received October 22, 2023; Revised January 30, 2024; Accepted November 25, 2024).

Abstract: The fabrication of anorthite-based ceramic foam filters with the function of filtering molten aluminum has been done using the replica method. To obtain the anorthite phase, kaolin and limestone were used as raw materials. Water glass acts as a deflocculant during the making of the slurry to lower the viscosity and improve the homogeneity of the suspension, with various weight percentages of 0.1%, 0.2%, and 0.3%. Samples were fired up to 1200ºC to obtain the anorthite phase. Characterization was conducted using SEM, EDS, XRD, and analysis of average pore area was performed using ImageJ software. Several tests were also carried out, including viscosity testing of the slurries, permanent linear change (PLC), and thermal expansion tests. An average pore area of 0.22 mm^2 to 0.28 mm^2 was obtained. Anorthite has been proven to be successfully obtained by firing up to 1200ºC. The water glass content does not affect the pore size and morphology but has a significant impact on the viscosity, permanent linear change, and thermal expansion. The more water glass content added to the slurry, the lower the viscosity and the higher the permanent linear change and thermal expansion percentage. The sample with 0.3 wt% of water glass results in the lowest viscosity of 1.25 cP, highest permanent linear change, and thermal expansion percentages of -4.19% and 0.67%.

Keywords: Ceramic foam filter; anorthite; water glass; aluminum

1. Introduction

Aluminum is lightweight and has high specific strength; hence the demand for aluminum is increasing everywhere[1]. The Ministry of Industry of Indonesia has targeted the production capacity of aluminum from 2025 and onwards at two million tons[2]. Therefore, aluminum scrap must be utilized to achieve this goal. One of the biggest challenges in the aluminum recycling industry is the presence of high-content inclusions. The inclusions can be in various forms and sizes, such as films, particles, or agglomerations that consist of oxides, borides, nitrides, carbides, and other combinations of elements. Typical inclusions in aluminum alloys are Al_2O_3, MgO, Al_2MgO_4, $CaSO_4$, TiB_2, Al_3Ti, and refractory bricks such as Al, Si, and O[3]. Inclusions are detrimental to the finished product because they reduce the mechanical properties, such as tensile and fatigue properties, and negatively affect the melt fluidity of the molten alloy[4]. Therefore, it is crucial to remove the inclusion content of aluminum alloys.

Removal of aluminum alloy inclusion can be done using fluxes, degassing, and filtration. Filtration is one of the most common processes to remove intermetallic and non-metallic inclusions during aluminum casting. Refining molten aluminum using the filtration method resulted in high homogeneity, improved machinability, improved mechanical properties, and the removal of metallurgical defects[5]. Due to the high temperature of molten aluminum, ceramics can be used for this purpose. Ceramics are not conductive, can withstand high temperatures, have high chemical stability, and are very strong[6]. Ceramic foam filters are commonly used for this purpose[7]. Most of them are produced in large quantities using the replica method, due to their simple applicability[8]. The replica method consists of soaking a polyurethane foam in a ceramic slurry, which is then burned to decompose the polyurethane and sinter the ceramic material[9]. During the making of the slurry, water glass plays a crucial role. Water glass acts as a deflocculant, which has the function of liquefying the slurry, thus making it less viscous[10]. Slurry with high viscosity can lead to a smaller coated area because of the difficulty of the slurry filling the polyurethane foam. On the other hand, slurry with a very low viscosity results in a very thinly coated sample that is prone to cracking during firing[11].

The most commonly used ceramic foam filters are made from calcined alumina (Al_2O_3). They have a high melting point, which also means a high sintering temperature of around 1600°C[12,13]. Therefore, this study aims to produce a ceramic foam filter that is made from a material that can be found in large numbers in Indonesia and can be produced with a lower sintering temperature than alumina.

Kaolin and limestone are the primary materials used in this study. Kaolin can be found in large quantities in Bangka Belitung[14]. Meanwhile, the biggest limestone reserve in Indonesia is in West Sumatra, with an amount of twenty-three thousand tonnes[15]. Kaolin is the source of SiO_2 and Al_2O_3[16], while limestone consists of calcium carbonate[17]. Calcium carbonate can be calcinated at temperatures above 800°C so that CaO is formed[18]. These raw materials are used so that the anorthite phase can be obtained. Anorthite is one of the phases that is present in the SiO_2–Al_2O_3–CaO phase diagram[19]. Anorthite has outstanding properties, such as a low thermal expansion coefficient, excellent thermal shock resistance, a low dielectric constant at high frequencies, and a low-density[20-22]. These properties are suitable for molten aluminum filtration. The anorthite phase can already be achieved at 1200°C[23].

2. Experimental

The starting materials that are used in this study are kaolin (obtained from kaolin mining industry of Sijuk, Belitung), limestone (obtained from Tuban), water, and water glass. To get the anorthite phase, the ratio of kaolin : limestone that is used is 73:27. The mixture of kaolin and limestone was put in a corundum-based pot mill with a capacity of 5 liters. 3 liters of water were also added to the pot mill. The mixture of kaolin, limestone, and water was wet-milled for 18 hours. After wet milling, more water and a variation of water glass are added to the mixture to make the slurries. The composition of slurries can be seen in Table 1.

Table 1. Composition of kaolin, limestone, water, and water glass.

Code	Kaolin:Limestone	Water (wt%)	Water glass (wt%)
A	73:27	67.44	0.1
B		67.36	0.2
C		67.28	0.3

After the slurries were made, the next step was soaking the polyurethane foam in the slurry. Polyurethane foam with 30 pores per inch was used in this study. After the foam is impregnated by the slurry, the wet sample is then put onto a flat surface of gypsum for drying. The samples were let to rest and dry for 7 x 24 hours. During the drying of the sample, excess water was absorbed by the gypsum below. Excess slurry was slowly removed from the sample by the force of gravity. After the samples were dry, they were then burned up to 1200°C in an electric furnace with a trajectory that can be seen in Fig. 1.

At first, the samples were burned with a heating rate of 2°C/min to reach 600°C. After that, a constant heat of 600°C is maintained for 30 minutes to decompose the polyurethane foam in the sample. A heating rate of 5°C/min is then achieved to reach 1200°C. At the final step, a constant heat of 1200°C is maintained for 60 minutes to obtain the anorthite phase. After burning, an anorthite-based ceramic foam filter can be further observed.

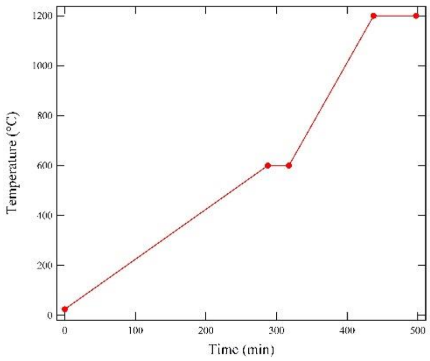

Fig. 1: Scheme of thermal treatment for anorthite samples.

To determine the properties of the anorthite-based ceramic foam filter, characterization and several tests were carried out. SEM (FE-SEM FEI Inspect F50), EDS, and XRD (Bruker, CuKα with a wavelength of 1.54 Å) were used to determine the chemical composition of the ceramic as well as prove the existence of the anorthite phase. Pore areas were calculated using the ImageJ software and the help of macroscopic images of ceramic foam filters. ImageJ software analyzes the area as well as the fraction of a phase or constituent through the color differences found in images. The image is rescaled to create a black and white (8-bit) image resolution, then a threshold setting is made to determine the boundaries of the retrieval area. The pore structure in this ceramic foam filter material has a different color from the framework or support, so that with the right threshold setting, the pore area can be calculated and determined. The tests that were done in this study were the viscosity test, the porosity test, the thermal expansion test, and the permanent linear change.

3. Results and Discussions

3.1 Chemical Composition

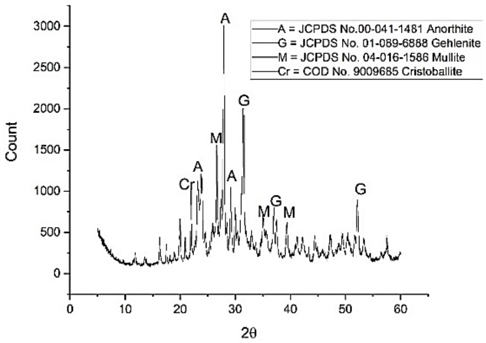

Fig. 2: XRD Result of anorthite ceramic filter.

To determine the chemical composition of the sample, X-ray diffraction and energy-dispersive X-ray spectroscopy were carried out. From Fig. 2, it is evident that anorthite has been successfully synthesized. Although the sample is not pure anorthite, other phases within the SiO_2-Al_2O_3-CaO phase diagram are also present. Those phases are gehlenite, mullite, and cristobalite. This is common due to the crystallization temperature of the respective phases. 950ºC is the crystallization temperature of gehlenite and anorthite[24)]. Mullite, on the other hand, can already be crystallized from an amorphous phase at 1000ºC[25)]. Due to the presence of amorphous silica, crystallization of cristobalite is triggered at a temperature of 1200ºC[26)].

At first, CaO is a result of decomposition at the firing temperature of 1050ºC. At the same temperature, anorthite starts to be synthesized with the formation of $CaSiO_3$. Finally, when the temperature is increased to about 1260ºC, the resulting XRD peaks match well with the characteristic peaks of anorthite (JCPDS: 41–1486). But to fully fabricate a single phase anorthite, a temperature of 1300ºC to 1450ºC is needed[27)].

According to the work of Kurama et al., layered aluminosilicate completely disappears due to the crystallization of the anorthite phase at 1200ºC. At this temperature, the crystallization process of anorthite occurs, as does the melting of gehlenite and layered aluminosilicate[23)]. The anorthite phase itself can already be obtained at 950ºC in a very dense condition. However, the temperature of 1200ºC is proven to be the best state at which the anorthite phase is formed[28)]. Anorthite formation in the sample makes the ceramic foam filter have good properties such as good thermal shock resistance, high creep resistance at high temperatures, and a very low thermal expansion coefficient[22)].

Table 2. EDS Result of anorthite ceramic filter.

Element	Unit	Water glass content (wt%)		
		0.1wt%	0.2wt%	0.3wt%
C	Wt%	00.94	01.31	01.22
O		28.64	34.17	27.24
Na		00.32	00.17	00.36
Al		11.35	18.61	12.32
Si		13.11	21.84	13.91
K		00.18	01.40	00.25
Ca		45.47	22.49	44.71

To obtain more insight on chemical composition of the ceramic filter, EDS was applied. According to the EDS result (Table 2), the most abundant elements that are present in the sample are Al, Si, Ca, and O. This result is very much in line with the XRD analysis, in which the identified phases are anorthite, gehlenite, mullite, and cristobalite. These phases are present in the SiO_2-Al_2O_3-CaO phase diagram. According to Yildrim et al., the EDS spectrum of an anorthite crystal consists of Al, Si, Ca, and O peaks[29)].

3.2 Morphology

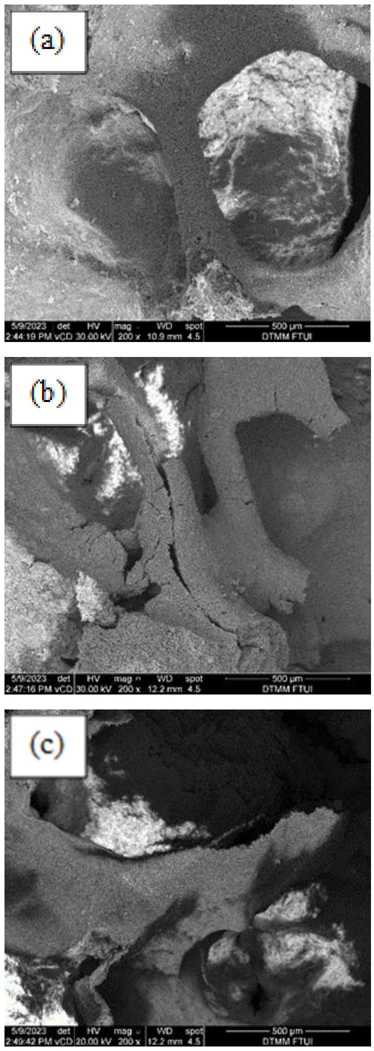

Fig. 3: SEM images (a) Sample A, (b) Sample B and (c) Sample C.

SEM and macroscope images were used to qualitatively observe the morphology of the sample. SEM was used to identify strut structures within the sample, and a macroscope was used to observe surface morphology. From the SEM images taken from each sample (Fig. 3), not many definitive features can be identified. Despite that, it is very clear that a strut with its pore structure can be seen. Therefore, it is evident that the ceramic foam filter takes almost the same form as its template, which is polyurethane foam.

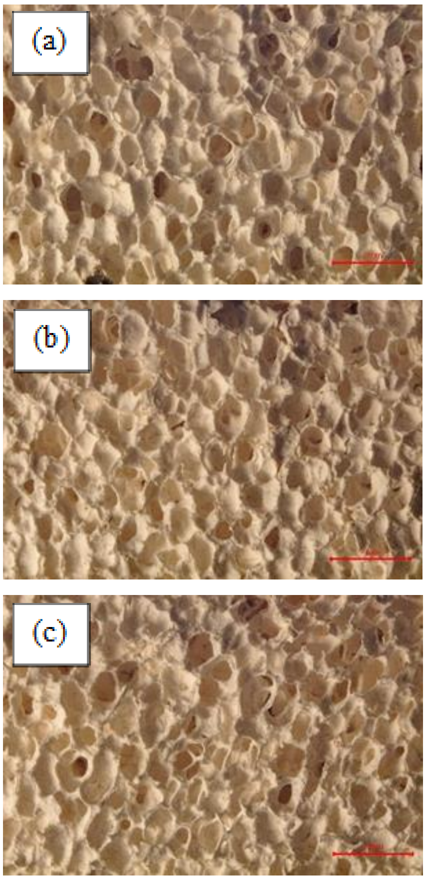

Fig. 4: Macroscopic images (a) Sample A, (b) Sample B and (c) Sample C.

Using the macroscope, a clearer image of the surface can be seen, revealing the strut with its pore structure as shown in Fig. 4. Although some of the pores are closed, it cannot be fully distinguished if the structure is an open pore structure or a closed pore structure purely from macroscopic observation. Using the ImageJ software, the mean area of the pores in each sample was calculated.

Table 3. Calculated mean area of pore using the ImageJ software.

Sample	Mean Area of Pore (mm^2)	Standard Deviation (mm^2)
A	0.223	0.035
B	0.202	
C	0.286	

From Table 3, no definitive pattern of the effect of the water glass on the pore size can be drawn. Although sample C with a water glass content of 0.3 wt% has the biggest pore area, no conclusive pattern can be derived from the data. This is because the pore size is not affected by the amount of deflocculant but rather by the shape of its template, which in this case is the PPI of the polyurethane foam[30)]

3.3 Viscosity

After adding water and water glass for the making of the slurry, a viscosity test is carried out using the Lehmann viscosimeter to determine the effect of the water glass content on the rheology of the slurry. The result of the test can be seen in Fig. 5 and Fig. 6.

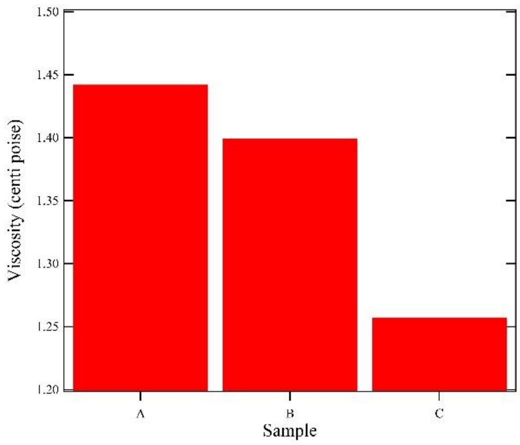

Fig. 5: Viscosity Result of the slurry.

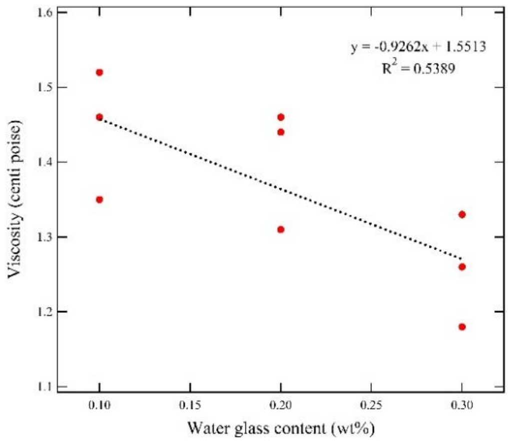

Fig. 6: Linear regression of the viscosity result of the slurry.

Figure 5 is a column chart that depicts the mean of viscosity numbers for three times of testing for each sample. Meanwhile, Fig. 6 is a linear regression chart for further understanding the effect of water glass content on the viscosity of the slurry. Water glass in this study acts as a deflocculant. The purpose of a deflocculant in a ceramic suspension is to remove interparticle attraction interaction as much as possible, which in effect increases the flowability of the slurry[31)]. With the decrease in viscosity, one of the resulting changes in the physical characteristics is that the fluidity increases[32]. From Fig. 6, it can be concluded that the more water glass is added to the slurry, the lower the viscosity becomes. According to the work of Evcin et al. who used different types of deflocculant in their study, the amount of water glass or sodium silicate can significantly alter the viscosity of the slurry. The lower the viscosity of the slurry, the more sodium silicate it contains[33].

3.4 Apparent Porosity, Water Absorption and Bulk Density

This test is carried out according to ASTM C20-00. Three different specimens for each sample code were weighted according to the procedure. The results can be seen in Fig. 7 and Fig. 8.

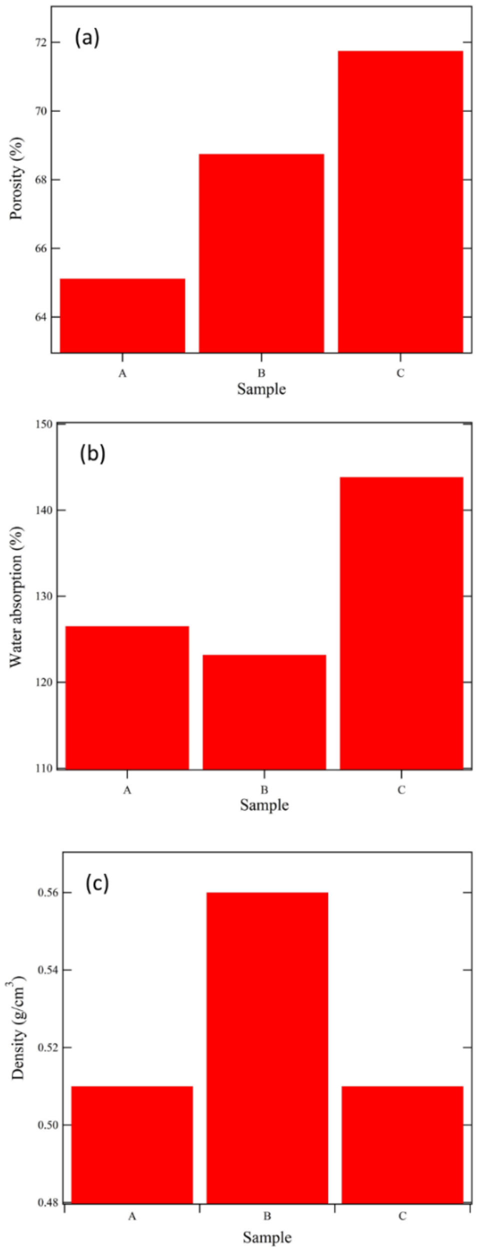

Fig. 7: (a) Porosity test result, (b) water absorption test result and (c) density test result.

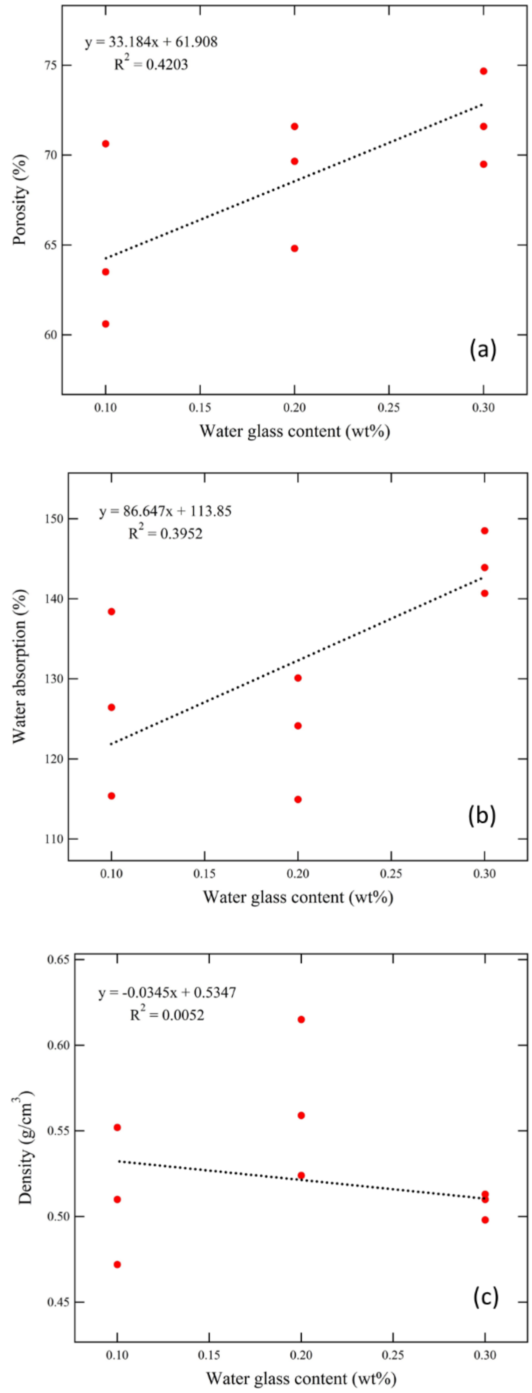

Fig. 8: Regression linear charts for (a) porosity, (b) water absorption and (c) density.

From Fig. 7(a), the porosity ranges from 65% to 71%. According to Liu et al., a typical ceramic foam has a porosity ranging from 70% to 95%[11]. This high percentage is because many types of porosity are present in a ceramic foam filter. The first type is called functional porosity. This type of porosity is surrounded by struts. Meanwhile, material porosity refers to pores that are present within the struts. And lastly, strut cavities are the biggest porosity within a ceramic foam filter. These cavities exist due to the decomposition of the template[12].

Besides that, it can be concluded from Fig. 8(a) that the more water glass is added, the higher the porosity percentage will be.

Looking at Fig. 7(b), the water absorption capacity of the sample ranges from 125% to 143%. This high number indicates that the sample is capable of absorbing more water than its weight. This number is the result of the amount of water absorbed divided by the weight of the sample. This high number means that there is a large amount of water retained within the pores of the sample[34]. From this explanation, it is evident that the sample has a high volume of open pores due to the high amount of water that is retained inside it[35]. From the linear regression chart of water absorption, it can be concluded that the high-water absorption capacity of the sample is proportionate to the amount of water glass added.

The density of the samples in Fig. 7(c) ranges from 0.51 g/cm^3 to 0.56 g/cm^3. The process of impregnating the polyurethane foam into the slurry is a crucial part of determining the density of the ceramic foam filter. Multiple impregnations are necessary to reach a certain amount of density. After impregnating the foam, excess slurry is usually removed using a centrifugal or a roller machine. But in this study, the excess slurry is slowly removed from the wet sample by the sheer force of gravity during the drying process on top of a gypsum surface. This is due to the very low viscosity of the slurry because visually, not that much slurry fully covers the polyurethane foam during impregnation. For this reason, mechanical removal of excess slurry is avoided to retain the remaining slurry that covers the foam. From Fig. 8(c), it can be concluded that water glass has an inverse effect on density, meaning that the more water glass is added, the less dense the sample will become.

Inferring from Fig. 8, it is evident that water glass has a proportionate effect on the apparent porosity and water absorption but has an inverse effect on density. This is because a high percentage of porosity means that the less the weight of the sample, the lower the density of the sample. But at the same time, a high percentage of porosity also means that there is more space for the water to be retained inside, and because of that, there is more capacity for water absorption[36].

3.5 Thermal Properties

The thermal properties that are tested in this study are permanent linear change and thermal expansion. During the permanent linear change test, the sample is heated slowly until it reaches the aluminum pouring temperature of 750°C and is maintained at that temperature for five hours. The measurement is then done after cooling down the sample. Meanwhile, in the thermal expansion test, the sample is directly exposed to a temperature of 750°C. The measurement is done simultaneously during heat exposure using a dilatometer. This test is carried out three times for each code sample with different specimens.

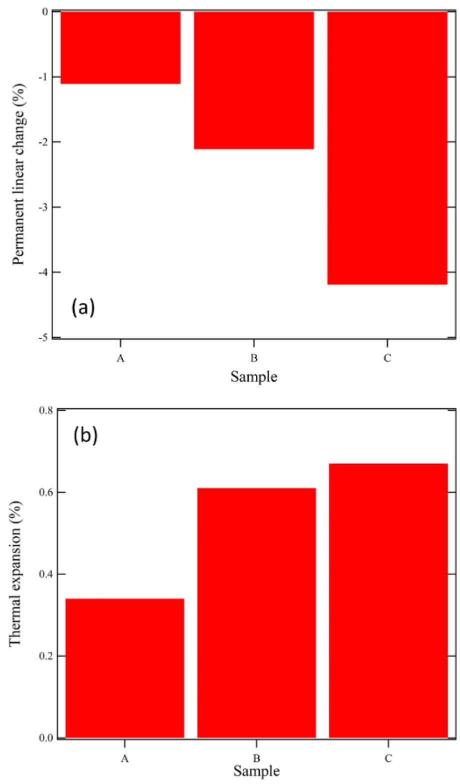

Fig. 9: (a) Permanent linear change test result and (b) thermal expansion test result.

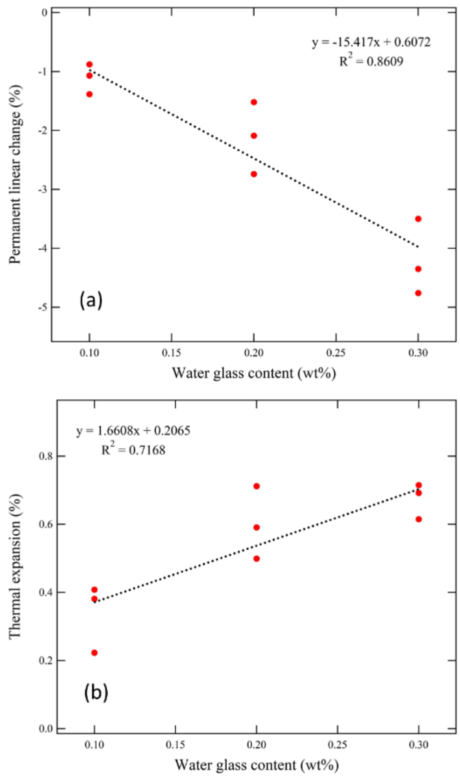

Fig. 10: Linear regression charts for (a) permanent linear change and (b) thermal expansion.

Inferring from Fig. 9(a) and Fig. 10(a), the percentages are negative in value. This means that the samples experienced shrinkage during the permanent linear change test at a temperature of 750°C. From Fig. 9 and 10, it is evident that the water glass content has a proportional effect on the permanent linear change and thermal expansion. This means that the more water glass is added to the sample, the more shrinkage it will experience during the permanent linear change test and the more expanded it will become. Since the less dense the material is, more changes can occur in its dimension because of heat exposure. This is aligned with the density results that were explained in the section before. This result is also in line with the study of Lindenthal et al. which also states that the more sodium silicate is added to the ceramic, the more it expands[37].

Conclusion

An anorthite-based ceramic foam filter has been successfully made using the replica method using kaolin and limestone as raw materials. The burning temperature of 1200^{o}C proved to be successful in synthesizing the anorthite phase. Water glass content or the amount of deflocculant does not affect the pore size of the ceramic foam filter, but rather the polyurethane foam. The ceramic foam filter has a large volume of open pores due to its high capacity for water absorption. Water glass has a proportional effect on apparent porosity, water absorption, thermal expansion, and permanent linear change. But on the other hand, water glass has an inverse effect on viscosity and density. The sample with 0.3 wt% of water glass has the best properties and results in the lowest viscosity of 1.25 cP, highest permanent linear change, and thermal expansion percentages of -4.19% and 0.67%.

Acknowledgements

The work was supported by a research grant from the Direktorat Inovasi dan Science Techno Park of Universitas Indonesia for the P5 Program in Program Pendanaan Inovasi 2023. ND-429/UN2.INV/PPM.00/2023. The authors would also like to thank Balai Besar Standarisasi dan Pelayanan Jasa Industri (BBSPJI) Keramik dan Mineral Nonlogam, Ministry of Industry, Bandung.

References

1) R. Yadav, S. Prakash Dwivedi, and V.K. Dwivedi, “Effect of casting parameters on tensile strength of chrome containing leather waste reinforced aluminum-based composite using rsm,” *EVERGREEN*, **9** (*4*) 1031–1038 (2022). doi:10.5109/6625716
2) “Rencana Induk Pembangunan Industri Nasional Republik Indonesia 2015-2035,” Jakarta, (2015). www.kemenperin.go.id.
3) G. Razaz, “Casting practices influencing inclusion distribution in Al-billets,” Karlstad University, (2013).
4) M. Máté, M. Tokár, G. Fegyverneki, and G. Gyarmati, “The comparative analysis of the inclusion removal efficiency of different fluxes,” *Archives of Foundry Engineering*, **20** (*2*) 53–58 (2020). doi:10.24425/afe.2020.131302.
5) A. Demir, “Fabrication of alumina ceramic filters and performance tests for aluminum castings,” in: Acta Phys Pol A, Polish Academy of Sciences, **134** 332–334 (2018). doi:10.12693/APhysPolA.134.332.
6) A.K. C, M. Reddy, and M.K. M, “Air jet erosion studies on aluminum-red mud composites using taguchi design,” *EVERGREEN*, **10** (*1*) 130–138 (2023). doi:10.5109/6781059
7) C. Voigt, E. Jäckel, F. Taina, T. Zienert, A. Salomon, G. Wolf, C.G. Aneziris, and P. Le Brun, “Filtration efficiency of functionalized ceramic foam filters for aluminum melt filtration,” *Metall. Mater. Trans. B*, **48** (*1*) 497–505 (2017). doi:10.1007/s11663-016-0869-5.
8) M. Bugdayci, Y. Üniversitesi, and G. Baran, “Effects of binding agents in the production of sic ceramic foam filters with replica method,” *J. Ceram. Process. Res.*, **22** (*5*) 510-516 (2021). doi:10.36410/jcpr.2021.22.5.510.
9) T. Fey, U. Betke, S. Rannabauer, and M. Scheffler, “Reticulated replica ceramic foams: processing, functionalization, and characterization,” *Adv Eng Mater*, **19** (*10*) 1-15 (2017). doi:10.1002/adem.201700369.
10) J. Gabriel Bruno da Silva, E. Fontenele Urano de Carvalho, N. Cabral Kuhnen, H. Gracher Riella, and A. Michael Bernardin, “Influence of Processing Water on Ceramic Suspension Viscosity,” in: *Qualicer 2008*, 119-124 (2008).
11) P.S. Liu, and Chen. G.F., “Fabricating Porous Ceramics,” in: *Porous Materials Processing and Applications, 1st ed., Elsevier Inc.*, Waltham, 221-302 (2014). doi: 10.1016/b978-0-12-407788-1.00005-8.
12) A. Bergin, C. Voigt, R. Fritzsch, S. Akhtar, L. Arnberg, C.G. Aneziris, and R.E. Aune, “Experimental study on the chemical stability of phosphate-bonded al2o3-based ceramic foam filters (cffs),” *Metall. Mater. Trans. B.*, **52** (*4*) 2008–2025 (2021). doi:10.1007/s11663-021-02144-3.
13) C.-B. Lim, H. Einaga, Y. Sadaoka, and Y. Teraoka, “Response of catalytic combustion-type sensor to different amounts of diesel particulate matter,” *Kyushu University Global COE Program Journal of Novel Carbon Resource Sciences*, **4** 1–7 (2011).
14) R. Julyana Manullang, M. Purnawan, D. Taufik, A. Ratnasari, and K. Noordiningsih, “Fabrication of cordierite ceramic foam filter by replication method,” *J. Indones. Ceram. Glass*, **30** (*1*) 35–45 (2021). doi: 10.32537/jkgi.v30i1.6855.
15) S. Habibie, A.H. Santosa Wargadipura, D. Gustiono, N. Herdianto, A. Riswoko, S. Nikmatin, and S. Clarke, “Production and characterization of hydroxyapatite bone substitute material performed from indonesian limestone,” *Int. J. Biomed. Eng. Sci.*, **4** (*1*) 11–23

(2017). doi:10.5121/ijbes.2017.4102.
16) R. Dewi, H. Agusnar, Z. Alfian, and Tamrin, “Characterization of technical kaolin using XRF, SEM, XRD, FTIR and its potentials as industrial raw materials,” in: J Phys Conf Ser, Institute of Physics Publishing, **1116** (*4*) 1-6 (2018). doi:10.1088/1742-6596/1116/4/042010.
17) I. Idris, B. Rustandi, T.R. Sulistiyani, A. Rahmat, and I.M. Sudiana, “Bioprospecting ureolytic rock bacteria for calcium carbonate precipitation inducer,” *EVERGREEN*, **9** (*4*) 962–972 (2022). doi:10.5109/6622882.
18) A. Razak, N. Mat Isa, S. Kinit, and S. Adzila, “Effect of calcination temperature on the properties of eggshell waste (ew) powder for biomedical application,” *EVERGREEN*, **10** (*2*) 782–791 (2023). doi:10.5109/6792828
19) S. Liu, and W. Ma, “Calcium-bearing minerals transformation during underground coal gasification,” *Minerals*, **9** (*11*) 1-19 (2019). doi:10.3390/min9110708.
20) M. Torman Kayalar, G. Erdogan, A. Yavas, S. Guler, and M. Sutcu, “Fabrication of porous anorthite ceramics using eggshell waste as a calcium source and expanded polystyrene granules,” *J. Polytech.*, **25** (*3*) 1235-1241 (2021). doi:10.2339/politeknik.911758.
21) C. Li, Y. Han, L. Wu, K. Chen, and L. nan An, “Fabrication and properties of porous anorthite ceramics with modelling pore structure,” *Mater Lett*, **190** 95–98 (2017). doi:10.1016/j.matlet.2016.12.131.
22) A. Harabi, S. Zaiou, A. Guechi, L. Foughali, E. Harabi, N.E. Karboua, S. Zouai, F.Z. Mezahi, and F. Guerfa, “Mechanical properties of anorthite based ceramics prepared from kaolin dd2 and calcite,” *Ceramica*, **63** (*367*) 311–317 (2017). doi:10.1590/0366-69132017633672020.
23) S. Kurama, and E. Ozel, “The influence of different cao source in the production of anorthite ceramics,” *Ceram Int*, **35** (*2*) 827–830 (2009). doi:10.1016/j.ceramint.2008.02.024.
24) Š. Csáki, T. Húlan, J. Ondruška, I. Štubňa, V. Trnovcová, F. Lukáč, and P. Dobroň, “Electrical conductivity and thermal analyses studies of phase evolution in the illite – caco3 system,” *Appl Clay Sci*, **178** 1-6 (2019). doi:10.1016/j.clay.2019.105140.
25) T. Ban, and K. Okada, “Crystallization of mullite and immiscibility in SiO_2 – Al_2O_3 system,” *Adv. Mater.,* ***93*** 483–486 (1994). doi:10.1016/b978-0-444-81991-8.50122-9.
26) F. Chargui, M. Hamidouche, H. Belhouchet, Y. Jorand, R. Doufnoune, and G. Fantozzi, “Mullite fabrication from natural kaolin and aluminum slag,” *Bol. Soc. Esp. Ceram. Vidr.*, **57** (*4*) 169–177 (2018). doi:10.1016/j.bsecv.2018.01.001.
27) C. Li, Y. Han, L. Wu, and C.A. Wang, “Synthesis and growth of anorthite crystal during in situ preparation of porous anorthite ceramics by foam-gelcasting,” *Int J Appl Ceram Technol*, **14** (*5*) 957–962 (2017). doi:10.1111/ijac.12727.
28) Z. Rajabi Mashhadi, and R. Naghizadeh, “Effects of temperature and duration of anorthite synthesis from mixtures of kaolin and calcite,” *J. Inst. Eng. (India): E.*, **102** (*2*) 227–238 (2021). doi:10.1007/s40034-021-00212-6.
29) H. Yildirim, Y. Azakli, M. Tarakci, and A. Capoglu, “The effect of surface polishing on the flexural strength of anorthite-based porcelainised stoneware,” in: *Acta Phys Pol A, Polska Akademia Nauk*, **127** (*4*) 1336-1341 (2015). doi:10.12693/APhysPolA.127.1336.
30) M.W. Kennedy, K. Zhang, R. Fritzsch, S. Akhtar, J.A. Bakken, and R.E. Aune, “Characterization of ceramic foam filters used for liquid metal filtration,” *Metall. Mater. Trans. B.*, **44** (*3*) 671–690 (2013). doi:10.1007/s11663-013-9799-7.
31) J.B. Rodrigues Nelo, A.P. Novaes De OLiveira, O.E. Alarcon, P. Pozzi, and F. Andreola, “Comparative Study of Deflocculation Mechanisms in Colloidal Clay Suspensions,” in: *Qualicer*, 283-300 (2002).
32) G. Zhakypova, S. Uderbayev, N. Saktaganova, G. Abyieva, A. Budikova, and A. Zhapakhova, “Properties of fine-grained concrete using ash of kazakhstan,” *EVERGREEN*, **10**(2) 830–841 (2023). doi: 10.5109/6792835
33) A. Evcin, “Investigation the effects of different deflocculants on the viscosity of slips,” *Sci. Res. Essays*, **6** (*11*) 2302–2305 (2011). doi: 10.5897/SRE10.686.
34) T. Sugiyama, H. Nagae, K. Suzuki, and K. Nakano, “Ceramic Brick with High Water Retentivity Prepared from Ceramic Waste and by Products,” in: *11th International Ceramics Congress, Trans Tech Publications Ltd*, 2235–2239 (2006). doi:10.4028/www.scientific.net/ast.45.2235.
35) T. Kato, K. Ohashi, M. Fuji, and M. Takahashi, “Water absorption and retention of porous ceramics fabricated by waste resources,” *J. Ceram. Soc. Jpn.*, **116** (*1350*) 212–215 (2008). doi:10.2109/jcersj2.116.212.
36) L. Uribe, J.D. Giraldo, and A. Vargas, “Effect of the operational conditions in the characteristics of ceramic foams obtained from quartz and sodium silicate,” *Materials*, **13** (*8*) 1-15 (2020). doi:10.3390/MA13081806.
37) J.W. Lindenthal, “Effects of the Rate of Heating on the Properties of a Low Temperature Vitreous Ceramic Body,” *Doctoral Dissertation*, The Ohio State University, (1959).